CHAPTER 7

ANALYSIS AND SIMULATION OF IPM GENERATOR DRIVING AN INDUCTION MACHINE

7.1 Introduction

In this chapter, the analysis and simulation results of the IPM generator driving a three phases, one horsepower induction machine will be presented. A schematic of the topology can be seen in Figure 7.1. Shunt capacitors placed at the terminals of the IPM are used to boost the terminal voltage and to supply reactive power. For the two machines used in the experiment, the use of the capacitors was not optional because it was found that the induction machine would not even start without the presence of the capacitors.

In the first part of the chapter, the dynamic and steady state equations used to model the induction machine will be presented. Next, the value of the parameters of the induction machine (and the methods used to determine the parameters) will be given. The comparison between the steady state experiment and calculated results will then be compared. Finally, simulated waveforms will be presented which show how the system behaves for three different types of load.

7.2 Derivation of Dynamic and Steady State Equations of a Squirrel Cage Induction Machine

The d q stator (after the stator resistance and core loss (see Figure 7.2)) and rotor voltage equations of the induction machine for the voltage can be written as

$$
\begin{aligned}
V_{qss} &= \quad {}_{ds} + p \quad {}_{qs} \\
V_{dss} &= - \quad {}_{qs} + p \quad {}_{ds} \\
V_{qr} &= r_r I_{qr} + (\quad - \quad {}_r) \quad {}_{dr} + p \quad {}_{qr} \\
V_{dr} &= r_r I_{dr} - (\quad - \quad {}_r) \quad {}_{qr} + p \quad {}_{dr} \ ,
\end{aligned}
\tag{7.1}
$$

where

$$
\begin{aligned}
{}_{qs} &= L_{lsm} I_{qsm} + L_{mm} (I_{qsm} + I_{qr}) \\
{}_{ds} &= L_{lsm} I_{dsm} + L_{mm} (I_{dsm} + I_{dr}) \\
{}_{qr} &= L_{lr} I_{qr} + L_{mm} (I_{qsm} + I_{qr}) \\
{}_{dr} &= L_{lr} I_{dr} + L_{mm} (I_{dsm} + I_{dr}) \ .
\end{aligned}
\tag{7.2}
$$

It is advantageous to have the equations entirely in terms of flux linkage and thereby eliminate the current terms.

Letting

$$
\begin{aligned}
L_{ss} &= L_{lsm} + L_{mm} \\
L_{rr} &= L_{lr} + L_{mm} \ ,
\end{aligned}
\tag{7.3}
$$

the flux linkage equations can be written as

It is also worth noting that the voltages V_{qr} and V_{dr} are equal to zero for the squirrel cage rotor used in this thesis (since the rotor windings are shorted together and can not support a voltage).

Now, the q axis terminal voltage of the stator may be found by recognizing that

$$\frac{V_{qs} - V_{qss}}{r_{sm}} = I_{qsmm} \ , \tag{7.8}$$

and

$$I_{qsmm} - \frac{V_{qss}}{R_c} = I_{qsm} \ . \tag{7.9}$$

Substituting Equation (7.8) into (7.9) and solving for V_{qss} gives

$$V_{qss} = \frac{R_c \, r_{sm}}{R_c + r_{sm}} \left(\frac{V_{qs}}{r_{sm}} - I_{qsm} \right) \ . \tag{7.10}$$

Substituting the value for I_{qsm} found in Equation (7.5) into (7.10) yields

$$V_{qss} = \frac{R_c \, r_{sm}}{R_c + r_{sm}} \left(\frac{V_{qs}}{r_{sm}} - \frac{1}{D} \left(L_{rr} \quad _{qs} - L_{mm} \quad _{qr} \right) \right) \ . \tag{7.11}$$

Equating Equation (7.11) with the solution for V_{qss} found in (7.7) and solving for V_{qs} gives

$$V_{qs} = \frac{r_{sm} \, L_{rr}}{D} \quad _{qs} + p \quad _{qs} \left(\frac{R_c + r_{sm}}{R_c} \right) + \left(\frac{R_c + r_{sm}}{R_c} \right) \quad _{ds} - \frac{r_{sm} \, L_{mm}}{D} \quad _{qr} \ . \tag{7.12}$$

The d axis terminal voltage of the stator may also be found by recognizing that

$$\frac{V_{ds} - V_{dss}}{r_{sm}} = I_{dsmm} \ , \qquad (7.13)$$

and

Substituting (7.11) into (7.14) and solving for V_{dss} gives

$$\frac{}{R + r}\left(\frac{V}{r} - I \quad\right) .$$

Substituting the value for I_{dsm} found in Equation (7.5) into (7.15) yields

Equating (7.16) with the solution for V_{dss} found in (7.5) and solving for V_{ds} gives

and the state equations may be written as

$$\begin{bmatrix} V_{qs} \\ V_{ds} \\ V_{qr} \\ V_{dr} \end{bmatrix} = \begin{bmatrix} \frac{r_{sm}L_{rr}}{D} + p\left(\frac{R_c + r_{sm}}{R_c}\right) & \left(\frac{R_c + r_{sm}}{R_c}\right) & -L_{mm}\frac{r_{sm}}{D} & 0 \\ -\left(\frac{R_c + r_{sm}}{R_c}\right) & \frac{r_{sm}L_{rr}}{D} + p\left(\frac{R_c + r_{sm}}{R_c}\right) & 0 & -\frac{r_{sm}L_{mm}}{D} \\ \frac{-r_r L_{mm}}{D} & 0 & \frac{r_r L_{ss}}{D} + p & (\quad - \quad_r) \\ 0 & \frac{-r_r L_{mm}}{D} & -(\quad - \quad_r) & \frac{r_r L_{ss}}{D} + p \end{bmatrix} \begin{matrix} qs \\ ds \\ qr \\ dr \end{matrix} . \qquad (7.18)$$

The equations for the shunt capacitors in the dq plane are given as

$$\begin{aligned} (-I_{qs} - I_{qsmm}) - \quad C V_{ds} &= p\, C V_{qs} \\ (-I_{ds} - I_{dsmm}) + \quad C V_{qs} &= p\, C V_{ds} \; . \end{aligned} \qquad (7.19)$$

At steady state, the rate of change of the states is zero, and Equations (7.18) and (7.19) may be reduced to

$$V \quad = \frac{r \quad L}{D} \quad + \quad \left(\frac{R \quad + r}{R}\right) \quad - \frac{r \quad L}{D}$$

$$V \quad = - \quad \left(\frac{R \quad + r}{R}\right) \quad + \frac{r \quad L}{D} \quad - \frac{r \quad L}{D}$$

$$0 = \frac{- r \quad L}{D} \quad + \frac{r \quad L}{D} \quad + (\quad - \quad)$$

$$0 = \frac{- r \quad L}{D} \quad - (\quad - \quad) \quad + \frac{r \quad L_{ss}}{D}$$

STD(648446062. TD(ss522 0 TD49 0 TD(+)Tj-0.1-1.1656 3Tj-0.1Tj-0.27 0.13 TD( )Tj-1.0

$$0 = \left(-I_{qs} - I_{qsm} - \frac{V_{qs}}{R_c}\right) - \quad C V_{ds}$$

$$0 = \left(-I_{ds} - I_{dsm} - \frac{V_{ds}}{R_c}\right) + \quad C V_{qs} \; .$$

The equations given in Equation (7.20), along with the two voltage equations of the IPM machine, i.e.

are the equations necessary to analyze the IPM feeding the induction motor (IPM-IM) when shunt capacitive compensation is present.

Due to the increased number of states created by the induction machine, no attempt at finding a closed form solution for the IPM-IM scheme was undertaken. Matlab's Fsolve

7.3 Induction Motor Parameter Determination

The determination of the parameters of the induction motor involves three different tests. They are the dc test, the blocked rotor test, and the no load test. The per phase, equivalent circuit of the induction motor is shown in Figure 7.3(a), where $X_1 = \omega L_{lsm}$, $X_2 = \omega L_{lr}$, and $X_m = \omega L_m$.

(a)

(b)

which reduces to

$$Z_{sc} = \frac{-r_r X_2 X_m + r_r X_m (X_2 + X_m)}{r_r^2 + (X_2 + X_m)^2} + r_{sm} + j\left(X_1 + \frac{X_2 X_m (X_2 + X_m) + r_r^2 X_m}{r_r^2 + (X_2 + X_m)^2}\right). \quad (7.24)$$

The real and imaginary parts may be written separately as

$$R_{sc} = r_{sm} + \frac{r_r X_m^2}{r_r^2 + (X_2 + X_m)^2}$$

$$X_{sc} = X_1 + \frac{r_r^2 X_m + X_2^2 X_m + X_2 X_m^2}{r_r^2 + (X_2 + X_m)^2} \quad . \quad (7.25)$$

For the no load test, the slip is very small and assumed to be zero and the equivalent circuit for the no load test is that of Figure 7.3(d).

The equivalent impedance is

$$Z_{nl} = \frac{V_1}{I_1} = R_{nl} + j X_{nl} \quad (7.26)$$

Which, in terms of the machine parameter is

$$Z_{nl} = r_{sm} + \frac{R_c j (X_1 + X_m)}{R_c + j (X_1 + X_m)} \quad . \quad (7.27)$$

By multiplying the numerator and denominator of the second term by the complex conjugate of the denominator (R_c - j (X_1 +X_m)) , Equation (7.27) can be reduced to

$$Z_{nl} = r_{sm} + \frac{R_c (X_1 + X_m)^2 + j R_c^2 (X_1 + X_m)}{R_c^2 + (X_1 + X_m)^2} \ . \qquad (7.28)$$

Separating Equation (7.28) into real and imaginary parts gives

$$R_{nl} = r_s + \frac{R_c (X_1 + X_m)^2}{R_c^2 + (X_1 + X_m)^2}$$

$$X_{nl} = \frac{R_c^2 (X_1 + X_m)}{R_c^2 + (X_1 + X_m)^2} \ . \qquad (7.29)$$

For a given operating frequency, the parameters X_m and R_c vary substantially as the supply voltage changes. Therefore, the no load test is performed for terminal voltages ranging from small to large. It is assumed that the leakage inductance and the stator and the rotor are equal, and thus the parameters to be solved for each condition are the core loss, the mutual impedance, the rotor resistance, and the leakage impedance (X_1 =X_2).

While the parameters of the IPM machine were made functions of the total stator current, the parameters of the induction motor are made functions of the peak mutual flux linkage of the induction motor. The plots of the core loss, mutual flux inductance L_m , leakage inductances L_{lsm} and L_{lr} , and rotor resistance r_r vs the mutual flux linkage λ_m are

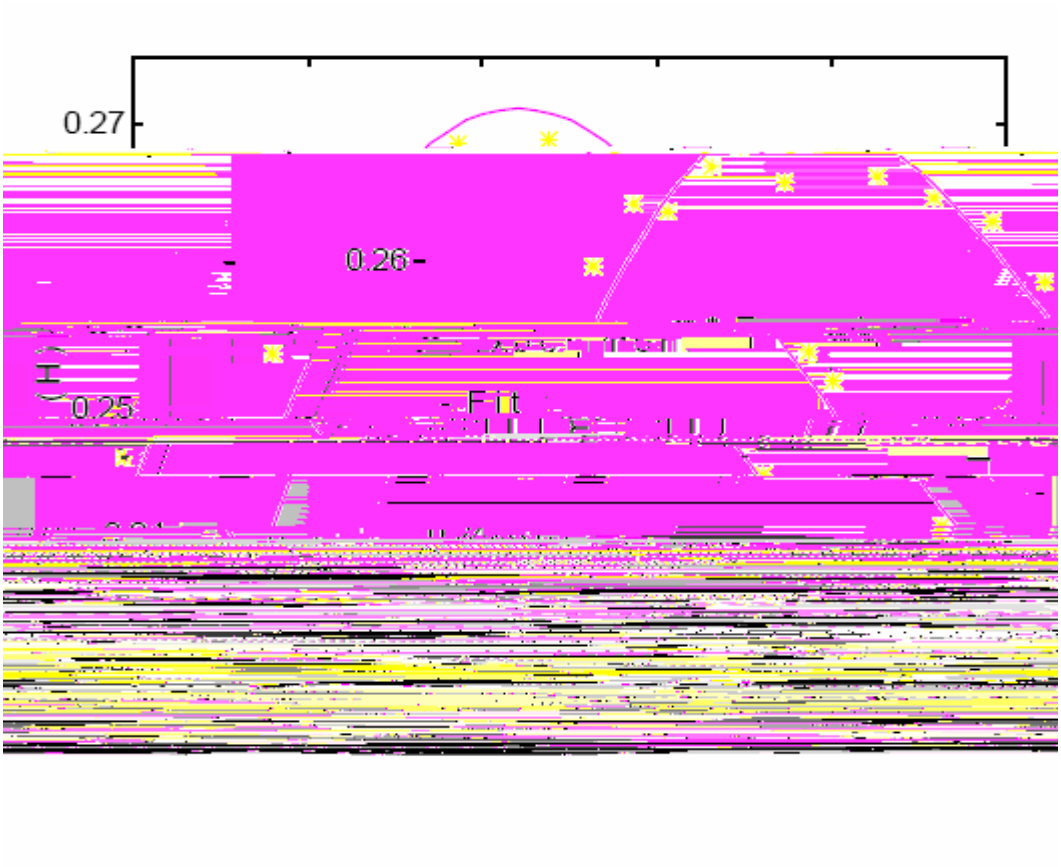

Figure 7.4. Plot of mutual inductance

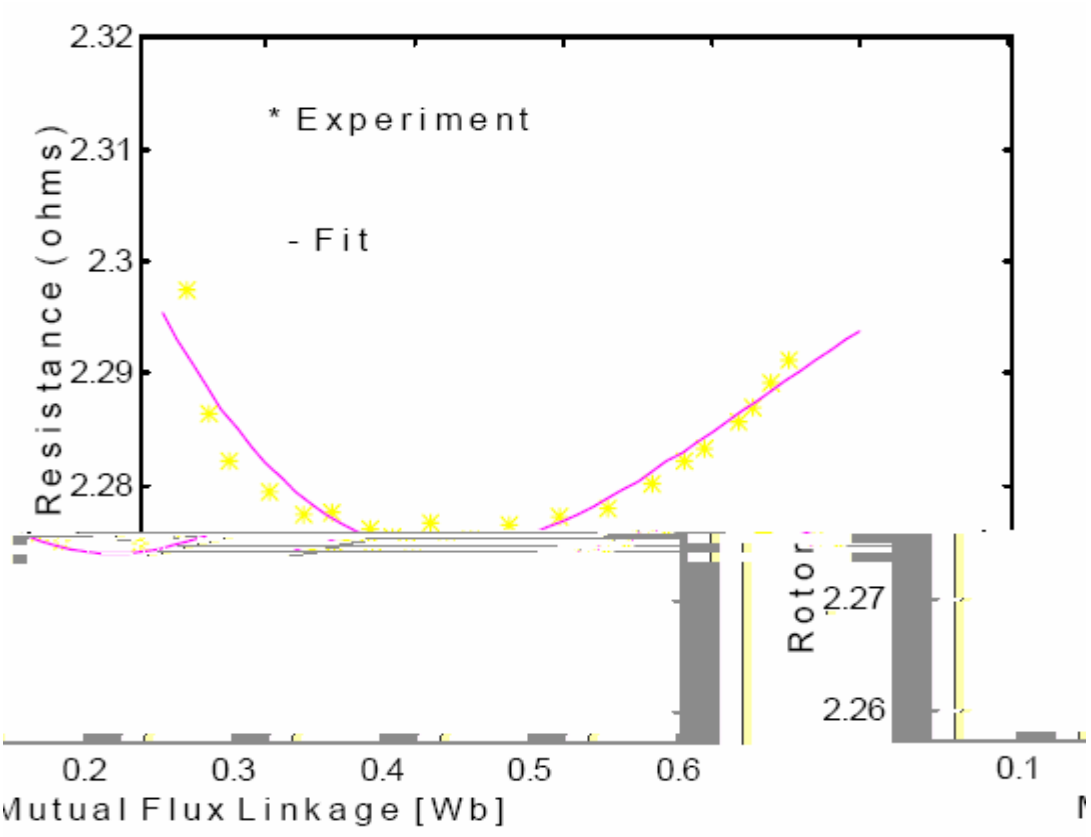

Figure 7.6 Plot of rotor resistance vs mutual flux linkage for induction motor

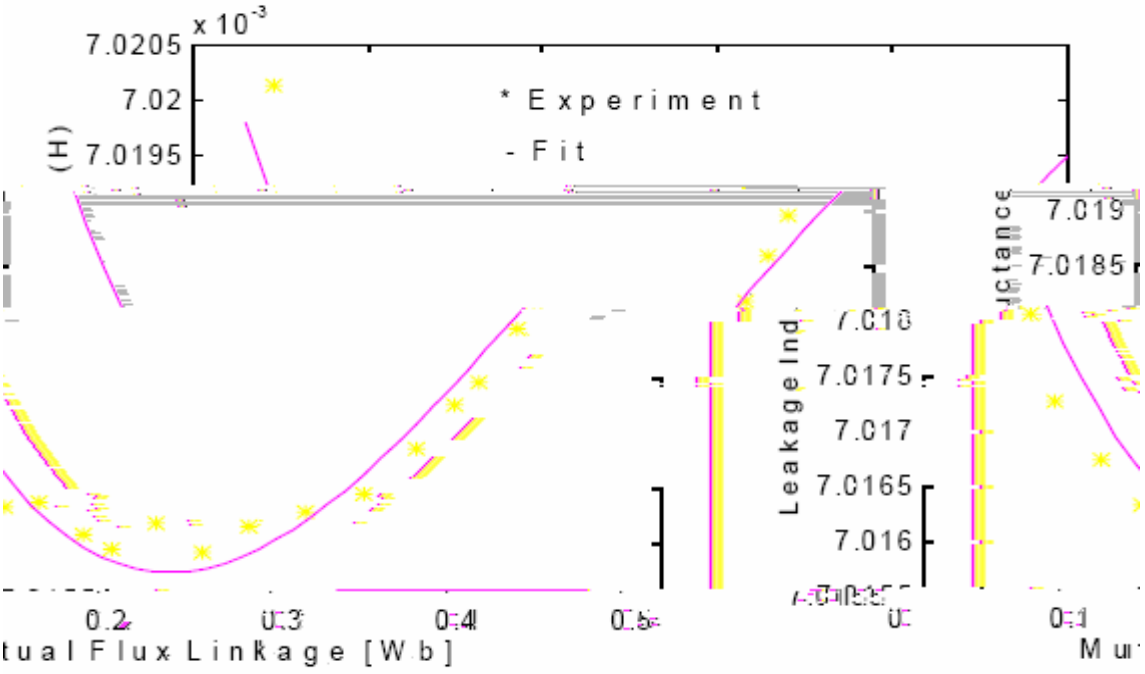

Figure 7.7. Plot of leakage inductance vs mutual linkage for induction

7.4 Measured and Calculated Steady State Results

This section involves presenting the measured and calculated steady state results of the IPM-IM scheme. For three different operating frequencies (30,45, and 60 Hz), the induction motor was allowed to run up to its no load operating scheme and the motor voltages, currents, and input power were measured. The per phase capacitance value used was 70 µF per phase Using a prony brake attached to the shaft of the induction motor, the torque was incrementally increased and the previously mentioned measurements were recorded for each load torque value.

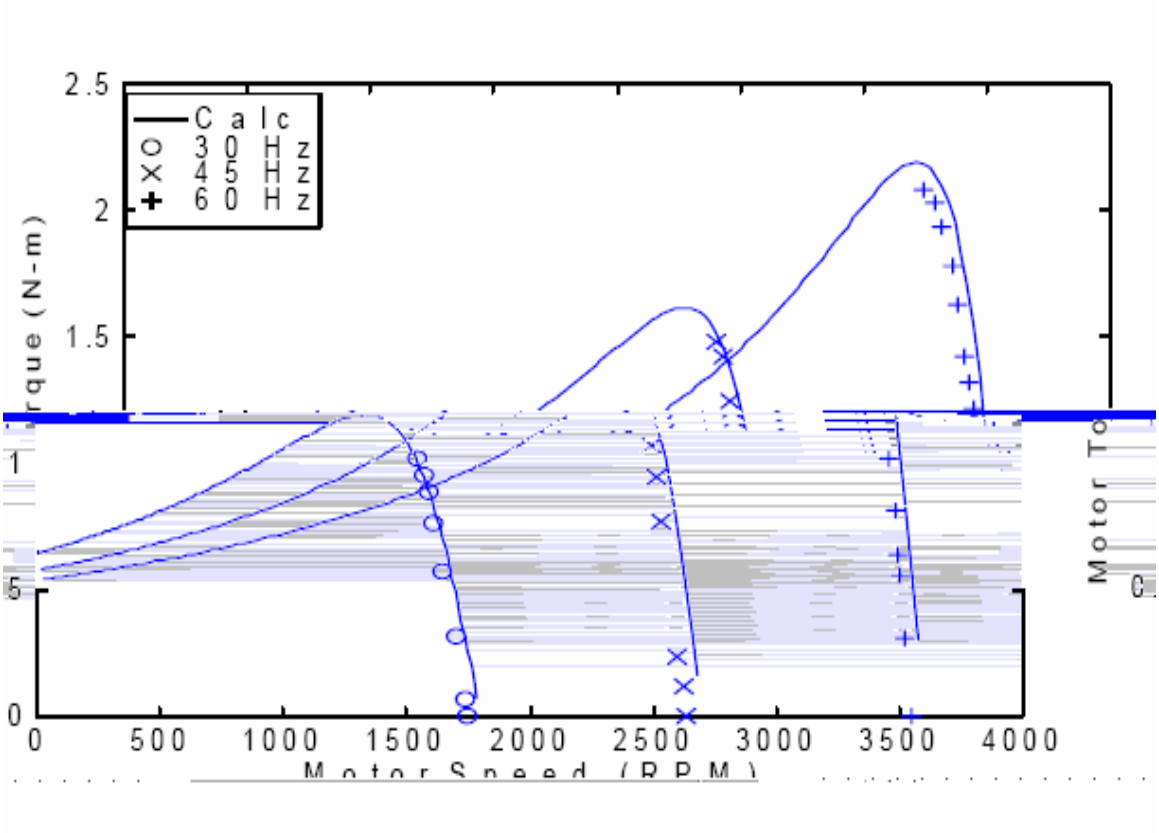

Figure 7.8(a) Measured and calculated load torque of induction motor for three different frequencies

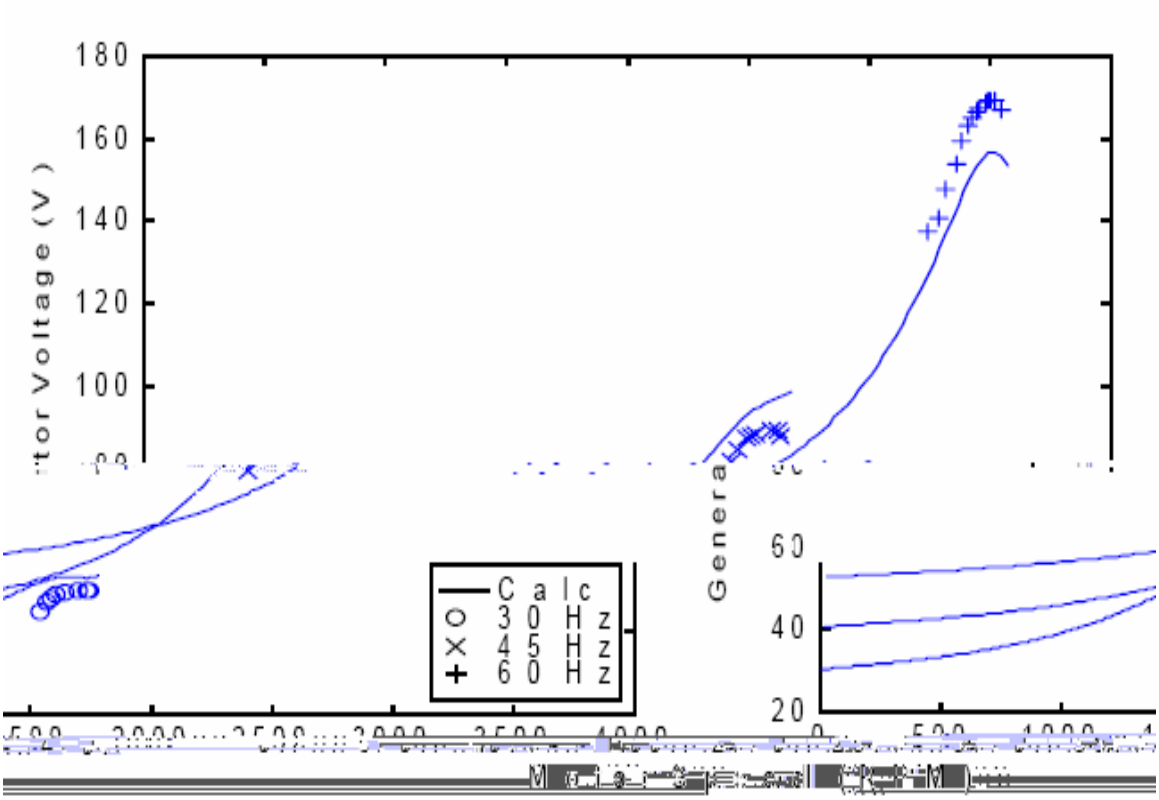

Figure 7.8(b). Measured and calculated peak generator output voltage vs motor speed for three operating frequencies

Figure 7.8(a) plots the measured and calculated output motor torque for three different frequencies. The maximum torques for the three different frequencies are substantially different from one another.

Figure 7.8(b) plots the generator (and motor) terminal voltage vs the speed of the induction motor. It can be seen that the voltage supply to the induction motor is clearly not constant and changes dramatically as the load (and therefore the speed) of the induction motor changes. It can be seen that, for 60 Hz, the maximum measured peak phase voltage is approximately 172 volts, which corresponds to an rms voltage of about 122 volts. The rated

voltage of the induction machine is 115 volts rms, so the 70 µF capacitor is adequate to provide a terminal voltage greater than or equal to the rated voltage over much of the operating range.

The plots shown in Figure 7.9(a) show the measured and calculated peak input motor current vs the motor speed for three different operating frequencies. It can be seen that the currents become very large when the motor speed is low. This, along with the fact that the torque becomes small (see Figure 7.8(a)), is why one would prefer not to operate in this region.

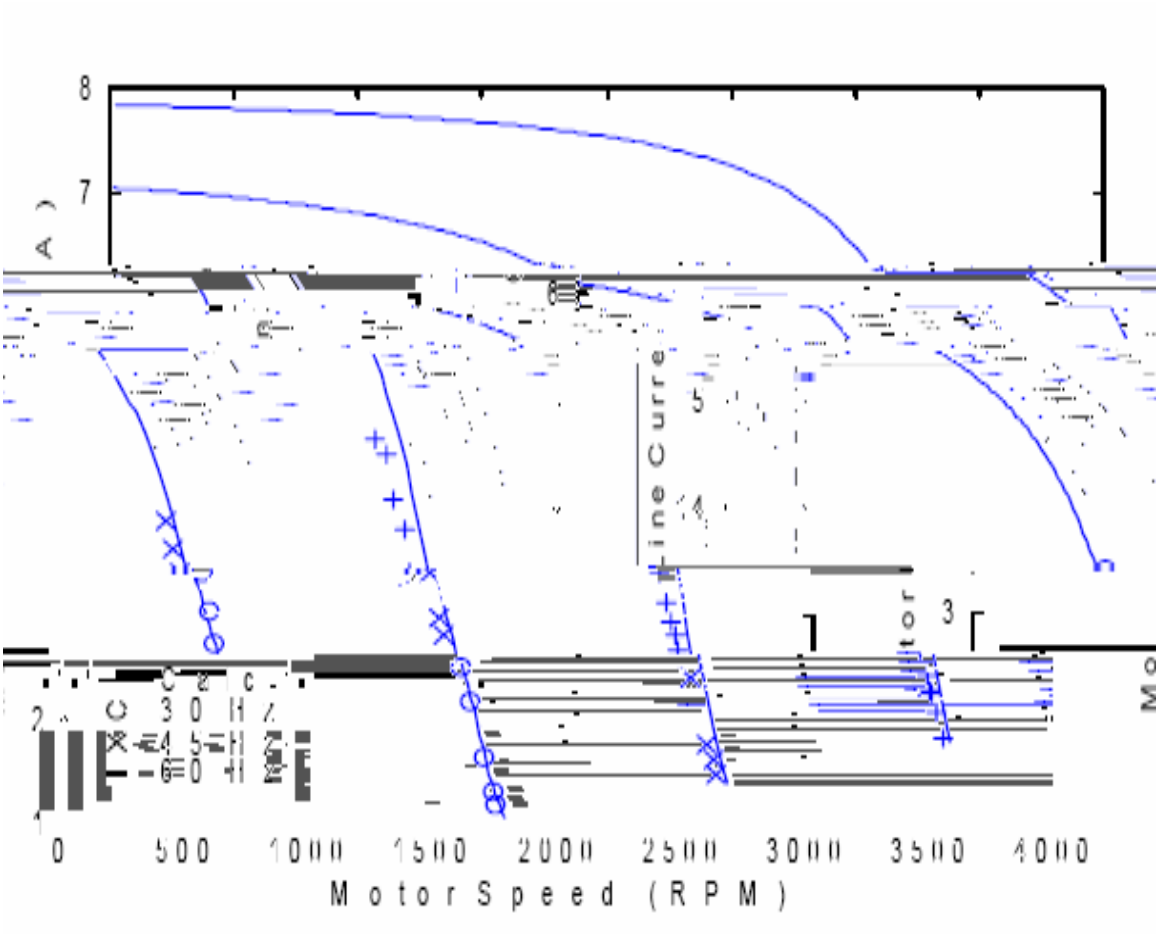

Figure 7.9(a) Measured and calculated peak motor input current vs motor speed

Figure 7.9(b) shows the variation of the input motor power factor vs the motor speed. For each of the operating frequencies, the maximum measured power factor is approximately 0.92. This is a reasonably good power factor, especially if one considers that it is obtained from an unregulated power source, i.e. the IPM machine. One of the drawbacks of the IPM machine is

Figure 7.10(a) shows the variation of motor input power vs the motor speed. It can be seen that the maximum measured power supplied to the induction machine is approximately 860 watts. The 2 horsepower IPM machine with the shunt capacitor compensation seems adequate to the task of supplying the necessary power required by the one horsepower (754 watts at output) induction machine.

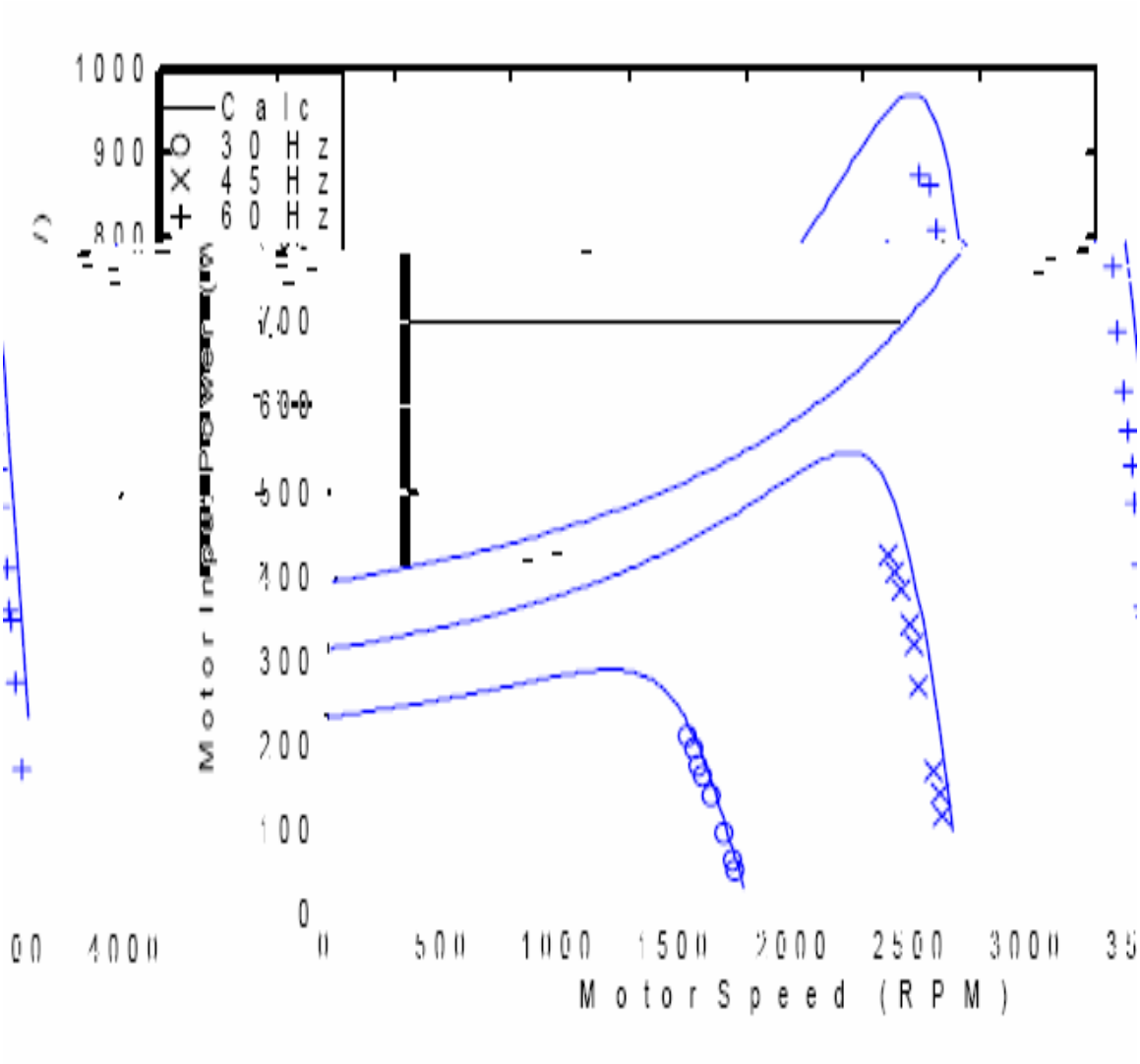

Figure 7.10(a). Measured and calculated motor input power vs motor speed for three operating frequencies

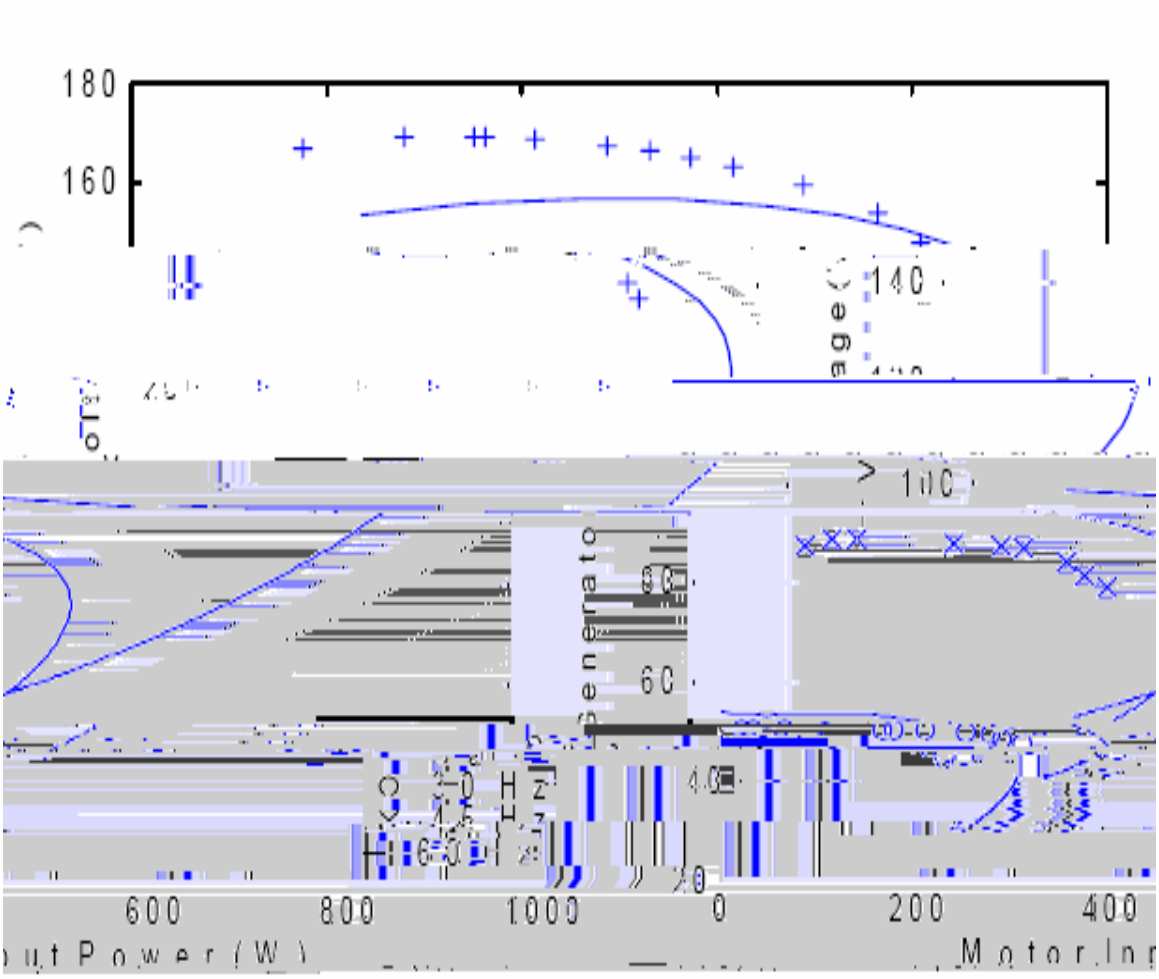

Figure 7.10(b). Calculated and measured peak phase generator voltage vs motor input power

Figure 7.10(b) plots how the generator (and motor) terminal voltage varies as a function of the motor input power and Figure 7.11 shows how the terminal voltage varies as a function of the motor input current. It can be seen from Figures 7.10(a) and 7.11, that the voltage regulation over much of the operating range is very good, i.e. the voltage does not change much. However, as the power approaches its maximum power point, and the current increases beyond 3.5 amperes, the voltage begins to fall rapidly.

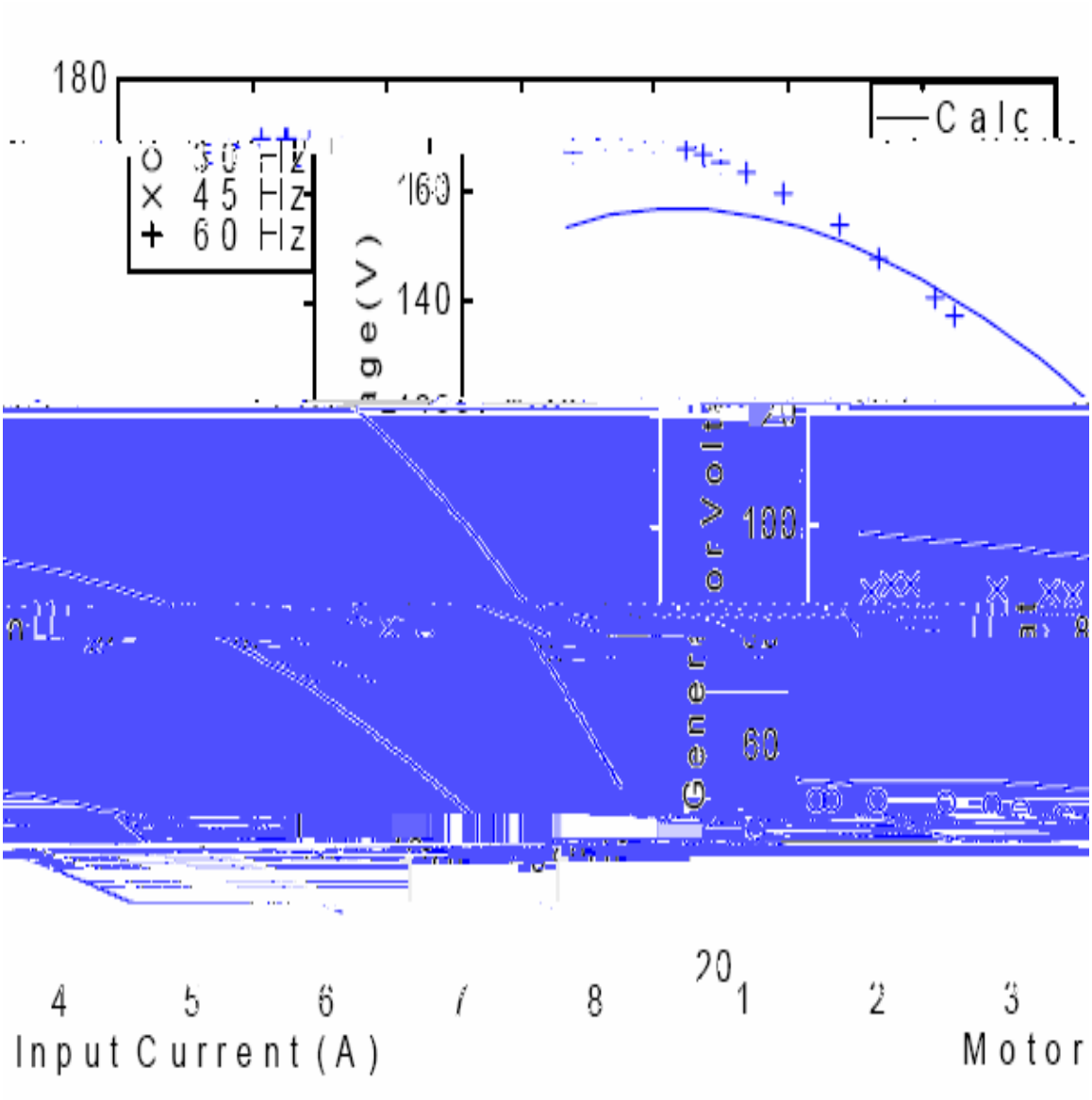

Figure 7.11. Measured and calculated peak generator voltage vs peak motor input current

7.5 Simulation of IPM-IM Scheme

In this section, the simulation of the IPM-IM system will be undertaken for three different types of loads. The first type of load will be a load torque which is proportional to the square of the motor speed. The second type of load will be where the load torque is proportional to the motor speed. The final type of load to be studied is when the load torque is proportional to the square root of the motor speed.

7.5.1 Simulation of IPM-IM Scheme When the Load is Proportional to the Square of the Motor Speed

The case when the load is proportional to the square of the motor speed models a fan or pump type load and is given by

$$T_l = T_0 + k_1 w_r^2 \ , \tag{7.31}$$

where T_l equals the load torque, and ω_r is the rotor speed. T_o equals the constant term which accounts, for the case of a pump load, for the amount of elevation which the fluid must be raised. This term is often referred to as the "head" of the system. This type of load will be referred to as a type a load. The induction motor used is rated at 1 horsepower (754 watts) and has a rated speed of 3450 rpm (361.3 rad/sec). The rated load torque may be solved as

—— ———— *m* .

A nominal value of 0.1 N-m was chosen for T_o. The coefficient k_1 term can be solved as

$$k_1 = \frac{T_{l\,rated} - T_o}{\omega_{rated}^2} = \frac{2.08 - .1}{361.3^2} = 1.52 * 10^{-5} \ . \qquad (7.33)$$

Thus, with k_1 and T_o known, the load torque for any particular operated speed may be solved using Equation (7-31).

As was the case for the steady state analysis of the system, the shunt capacitors used for the simulation were 70μF per phase. The operated speed of the generator was 377 rad/sec.

Figure 7.12 shows the generator current, terminal voltage, motor stator current and motor rotor current waveforms, respectively. It can be seen that the initial currents of the generator current are approximately 6 amperes during the transient response during which the motor speed is increasing, and come to a steady state value of approximately 5 amperes. The generator phase voltage starts at a small value of approximately 50 volts and builds to a final value of 150 volts. The 150 volts (106 volts rms) is only slightly lower than the 115 volt rms value for which the induction machine was designed to operate at, and, thus, there is a relatively good match between the IPM-IM topology with this type of load for the capacitor values chosen. The motor input current (Figure 7.12(c)) shows the basic form as that of the generator currents. The difference is that the magnitude is slightly less, due to the capacitor drawing off some of the current. Figure 7.12(d) shows the current flowing in the

rotor. The initial currents are approximately 7.5 amperes. At steady state, the rotor current is almost 4 amperes. The frequency of oscillation of the rotor current at steady state is much slower than the transient period since its magnitude is dependent largely upon the difference between the electrical supply frequency and the actual rotor speed.

Figure 7.13(a) shows the buildup of the motor speed as a function of time. It can be seen that the final motor speed is approximately 355 rad/sec (3,390 rpm). This speed is slightly below the rated speed of the machine (3,450 rpm). Figure 7.13 (b-c) shows the load torque of the motor and the electromagnetic torque of the motor respectively. The final output load torque is approximately 2.0 N-m which, at a speed of 355 rad/sec gives a power output of 710 watts (.94 horsepower). If the objective was to obtain a one horsepower output, then optimization of the system, assuming all other variables remain constant, would ultimately result in slightly increasing the size of the capacitor. Finally, Figure 7.13(d) shows how the electromagnetic and load torques vary as a function of the motor speed. It can be seen that the average value of the electromagnetic torque (the middle of the envelope of oscillation) is always larger than the load torque. This difference in magnitude pulls the motor speed up into its final steady state value. The characteristics of this pump type load are thus a good match for the given IPM-IM topology.

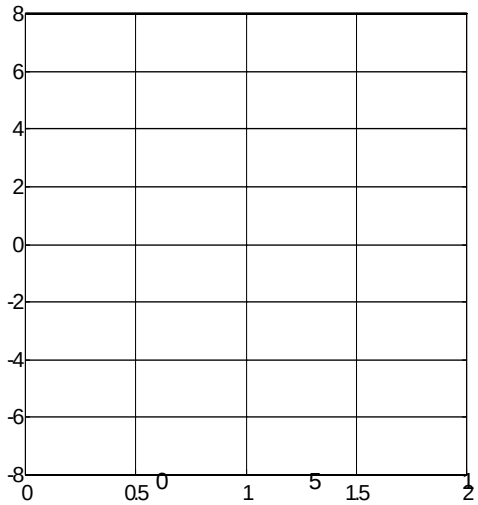

0.5 0 5 1 1

(a) (b)

(c) (d)

Figure 7.12. Simulated waveforms of (a) generator current, and (b) generator voltage, (c) motor imput (stator) current, (d) motor rotor current for IPM-IM topology operating under fan type load

0 5 -

7.5.2 Simulation of IPM-IM Scheme When the Load is Proportional to the Motor Speed

The case when the load is proportional to the motor speed (type b load) is

$$T_l = T_0 + k_2 w_r \ , \tag{7.34}$$

where T_l equals the load torque calculated in section 7.5.1, i.e. 2.08 N-m, T_o for this section will be chosen to be equal to zero. The coefficient k

builds up, the magnitudes of each increase steadily. The generator voltage, as seen in Figure 7.16(b), is almost 150 volts (as compared

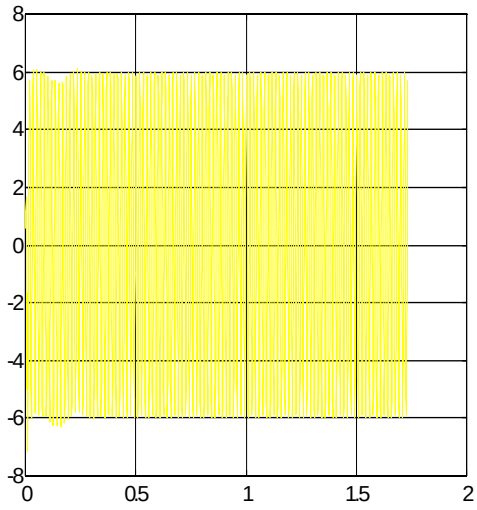

(a) (b)

(c) (d)

Figure 7.14. Simulated waveforms of (a) generator current, (b) generator voltage, (c) motor input current, and (d) motor rotor current for IPM-IM topology operating under type b load

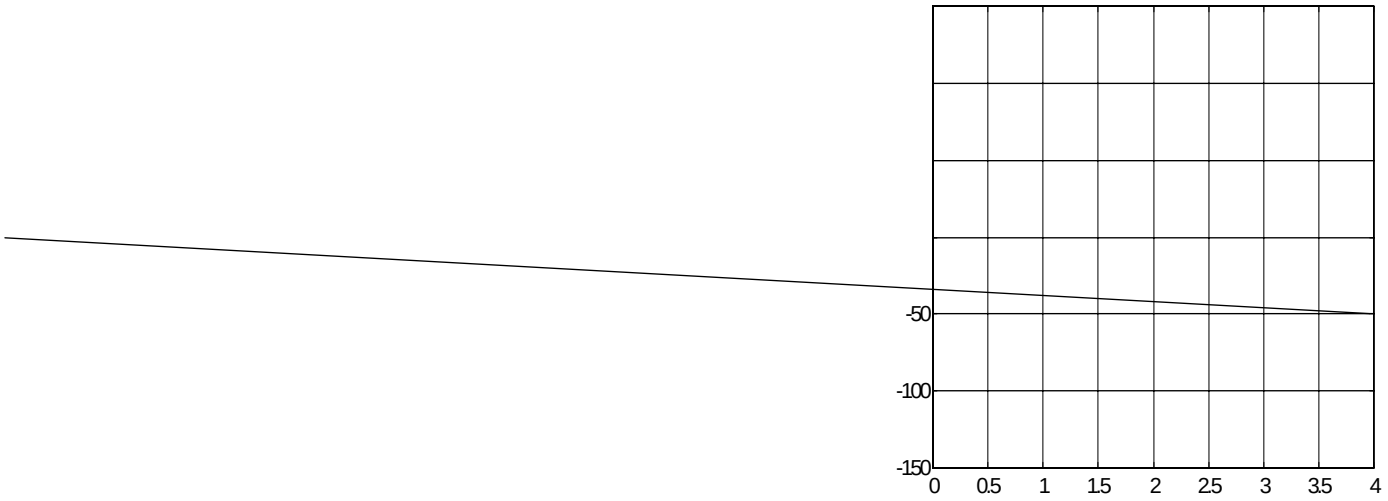

(a) (b)

(c) (d)

Figure 7.16. Simulated waveforms of (a) generator current, (b) generator voltage, (c) motor input current, and (d) motor rotor current for IPM-IM topology operating under type b load

7.5.3 Simulation of IPM-IM Scheme When the Load is Proportional to the Square Root of the Motor Speed

Figure 7.18 (a-d) shows the simulated waveforms of the generator current , generator phase voltage, induction motor input current and motor rotor current when the IPM-IM

(a) (b)

(c) (d)

Figure 7.18. Simulated waveforms of (a) generator current, and (b) generator voltage, (c) motor input (stator) current, (d) motor rotor current for IPM-IM topology operating under type jT*)TjT7oad08 TcETq1 i 86.1 45vef4 214.92 214.56 reW nqvef6740708.72

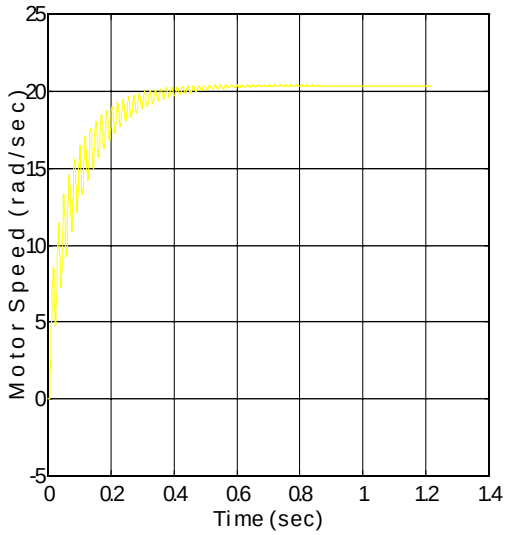

(a)

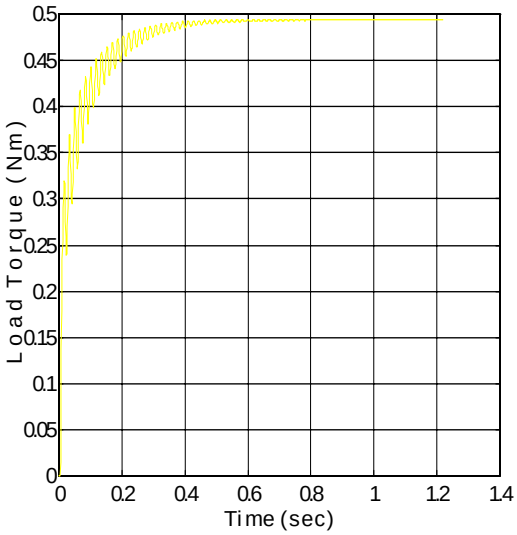

(b)

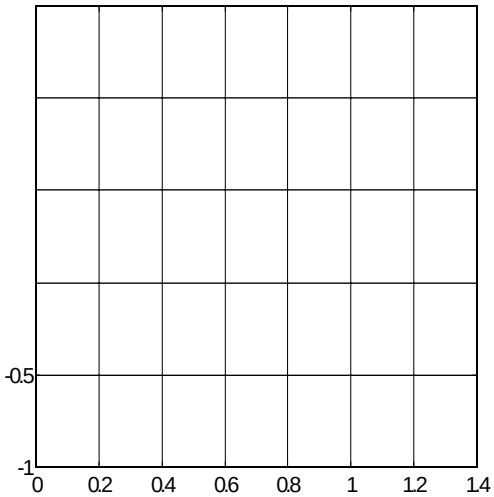

(c)

(d)

Figure 7.19. Simulated waveforms of (a) motor speed, (b) load torque, (c) motor electromagnetic torque, (d) electromagnetic and load torque vs motor speed for IPM-IM topology operating under type c load